



Theory Research of Curved Surface Reflection RIM-FOS under the Typical Optical Fiber Beam Structure

Hao Hu^a, Liqiong Zhong^{*b}

^aSchool of Mechanical Engineering, Guizhou University, Huaxi District, Guiyang 550025, China

^bSchool of Mechanical Engineering, Guiyang College, No.103, Jianlongdong Road, Nanming District, Guiyang 550005, China
haohu0105@126.com

This paper has completed the theoretical modeling of the cured surface reflection RIM-FOS under the typical optical fiber bundle structure. Firstly, the modeling of the fiber's axial symmetry distribution structure is made by analytical method to get the intensity modulation function M . Then the modeling of the fiber's coaxial distribution structure is made by analytical method to get its intensity modulation function M . Finally, the simulation experiment about the mathematical model of the two typical optical fiber beam structure is conducted to get the corresponding P- M curve when the variables d , r , l change. The simulation results show that the relationships between the variable d , r , l and the received light intensity under different fiber bundle structures indicate that the calculation results of the mathematical model are in conformity with the actual situation. Finally, it is concluded that detection range is similar to the detection sensitivity under the two typical optical fiber bundle structures, which provides a good theoretical basis for practical design of RIM-FOS.

1. Introduction

Today, Reflective intensity modulated fiber optic sensors RIM-FOS has occupied a very important position in the field of fiber optic sensing. Whereas, the RIM-FOS is one of the products that are most widely used and easiest to implement, to be the research priority of many scholars (Erik et.al, 2012; Faria, 1998; García et.al, 2010; Nevshupa et.al, 2013; Zawawi et.al, 2013). It's believed that by the further research and development of the RIM-FOS, this kind of sensor technology will have a broader prospect of application.

Therefore, it is very necessary to analyze intensity modulation mechanism of RIM-FOS. Such mechanism has already been studied by some of scholars, for example, Jianli zheng derived the theoretical model of optical fiber displacement sensor, and presented the normalized characteristic curves for the test and theory (Zheng and Albin, 1999). Jose Branda Faria established the model for double-circled fiber bundle by means of geometric method and Gaussian method, while analyzed the characteristic curve of "normalized distance--normalized optical power" (Brandao, 2000). Puangmali constructed the mathematical models for front end curving of light, as well as the case that the same optical fiber is used for transmitting and receiving optical fibers (Puangmali and Pinyo, 2010) (Puangmali and Pinyo, 2011).

The literatures on above intensity modulation mechanism of RIM-FOS were conducted under the premise that the surface was not deformed, yet the studies on bending deformation are relatively less, Because it is difficult to establish its mathematical model under this kind of circumstance, and the traditional geometric modeling method is hard to achieve. RIM-FOS which is based on the curved surface reflection is relatively common in the practical application, so systematically theoretical research is needed on this situation. For this reason, this paper plans to research the intensity modulation model of RIM-FOS which is based on the curved surface reflection by analytic method under the typical distribution structures such as fiber's axial symmetry distribution and fiber's coaxial distribution, and so on, to provide certain theoretical basis for the development of this sensor type.

2. Working principle

As shown in Figure 1, it is a schematic structure of reflective intensity modulated sensor distributed in fiber-optic axisymmetric way. When the sensor operates, the light after coupling passes into TF and irradiates onto the elastic sheet, and part of reflected light of elastic sheet enters to RF. Under the external pressure P, the elastic sheet at the same time presents the axial and radial deformation, while the deformation occurs in the axial direction would shorten the distance d between the elastic sheet and RF, then the light intensity received by RF changes. In such a way that the output light intensity of RF will change with the distance d between the elastic sheet and fiber, and thereby reflecting the deformation of the elastic sheet based on the change amount of the received light intensity, and changes ΔP of external pressure can finally be derived.

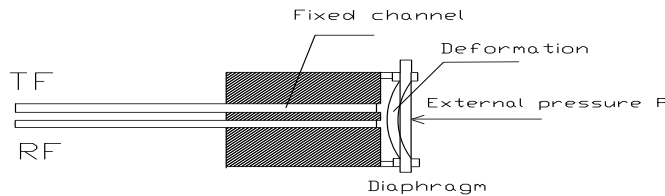


Figure 1: Sensor structure diagram

3. Analytical Method Modeling

3.1 Optical Fibers with Axially Symmetric Distributions

The exact math model can be got by the three-dimensional analytical method modeling under this circumstance. In many industrial applications, there are no too many requirements for the calculation accuracy of the model, so the calculation can be simplified. Without loss of generality, this paper will simplify the math modeling of the axially symmetric distributions of TF and RF, and its computational principle diagram is as shown in the figure 2. TF is the incident optical fiber in the figure, RF is the receiving optical fiber, I_{AB} , I_{CD} are the boundary emergent lights, and I_{BE} , I_{DF} are the lights after the curved surface reflection. Figure 3 displays the position relations between the end surface EF of the reflected light cone and the receiving optical fiber, which is divided into three cases shown in the figure and only the receiving optical fiber can output light signal when they are compatible or intersecting. During the modeling, assumptions are as follows.

- ① The emergent light field intensity of the incident optical fiber TF is uniform distribution;
- ② Under the uniform pressure P, when the radius R_B of the elastic diaphragm is much longer than the radius of the optical fiber, the deflection equation is regarded approximately in line with the simplified formula as follows after the deformation of the elastic diaphragm:

$$w(x) = A(R_B^2 - 2x^2) \tag{1}$$

In which, A is the deformation coefficient of the elastic diaphragm, $w(x)$ is the deflection that has a distance of x from the center of the diaphragm, $D = (Et^3)/(12(1 - \mu^2))$, E is the modulus of elasticity of the elastic diaphragm, t is the thickness of the elastic diaphragm, and γ is the Poisson's coefficient.

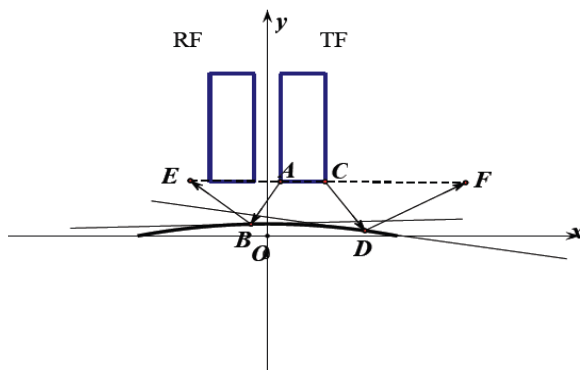


Figure 2: Symmetrical distribution of fiber

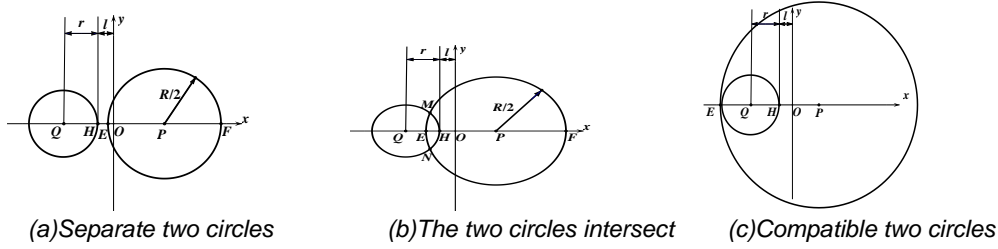


Figure 3. The position of the reflected light cone and RF

By analytic calculation, the light intensity modulation function M that is as shown in formula (2) can be got:

$$M = \begin{cases} 0 & |x_E| \leq l \quad (x_E < 0) \\ 4\mu_0\mu_1 \left[\frac{\pi}{2} R^2 + R^2 \arcsin \frac{x_M - (R + x_E)}{R} + [x_M - (R + x_E)] \sqrt{R^2 - [x_M - (R + x_E)]^2} \right. \\ \quad \left. + \frac{\pi}{2} r^2 - r^2 \arcsin \frac{x_M + (r + l)}{r} - [x_M + r + l] \sqrt{r^2 - [x_M + r + l]^2} \right] / \pi R^2 & l < |x_E| < 2r + l \quad (x_E < 0) \\ 4\mu_0\mu_1 r^2 / R^2 & |x_E| \geq 2r + l \quad (x_E < 0) \end{cases} \quad (2)$$

In the formula, r is the radius of the optical fiber, $2l$ is the distance between the two optical fibers, NA is the numerical aperture of the optical fiber, R_B is the radius of the diaphragm, and d is the initial distance between the optical fiber and the diaphragm. The value of x_E , x_M , R respectively is:

$$x_E = (k_5 m + d - n) / k_5 \quad (3)$$

$$x_M = x_N = (x_E^2 + 2R x_E - 2rl - l^2) / 2(R + x_E + r + l) \quad (4)$$

$$R = x_F - x_E = (k_6 h + d - u) / k_6 - (k_5 m + d - n) / k_5 \quad (5)$$

The gradient of the reflection ray i_{BE} and i_{DF} respectively are k_5 and k_6 .

3.2 Coaxial distribution of optical fiber

In the optical fiber’s probe designing, people often adopt the distribution structure that output optical fibers are coaxial with the reflective surface. This kind of distribution structure is compact and regular. Now by using the theory of analytic method, the intensity modulation model of this typical distribution structure is analyzed. As is shown in figure 4 below, it is the brief structure diagram of the output optical fibers and the coaxial reflective surface. In the figure, i_{AC} and i_{BD} are the boundary emergent lights. i_{CE} and i_{DF} are the lights after the curved surface reflection. The position relations between the end surface EF of the reflected light cone and the receiving optical fiber are as shown in figure 5 below.

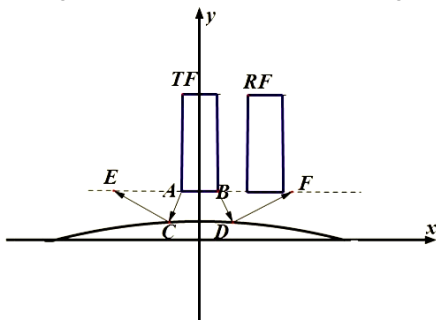
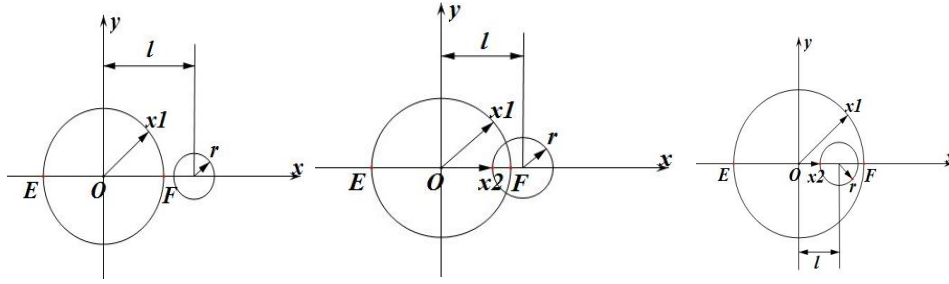


Figure 4: Coaxial distribution of fiber



(a) Separate two circles (b) The two circles intersect (c) Compatible two circles

Figure 5. The position of the reflected light cone and RF

Also by analytic calculation, the light intensity modulation function M under this case that is as shown in formula (6) below can be got:

$$M = \begin{cases} 0 & (x_1 \leq l - r) \\ \mu_0 \mu_1 \frac{\left[r^2 \arcsin\left(\frac{x_2 - l}{r}\right) + (x_2 - l)\sqrt{r^2 - (x_2 - l)^2} + \frac{\pi}{2}(r^2 + x_1^2) - x_1^2 \arcsin\frac{x_2 - x_1}{x_1} - x_2 \sqrt{x_1^2 - x_2^2} \right]}{\pi x_1^2} & (l - r < x_1 < l + r) \\ \mu_0 \mu_1 \frac{r^2}{x_1^2} & (x_1 \geq l + r) \end{cases} \quad (6)$$

In the formula, r is the radius of the two optical fibers, l is the distance AB between the end surfaces of the two optical fibers, NA is the numerical aperture of the optical fiber, d is the initial distance between the optical fiber and the diaphragm, R_B is the radius of the diaphragm, and x_1, x_2 respectively is $x_2 = \frac{x_1^2 - r^2 + l^2}{2l}$,

$$x_1 = \frac{d - n}{k_3} + m, \text{ in which } k_3, m, n \text{ respectively is}$$

$$k_3 = \frac{k_1 k_2^2 + 2k_2 - k_1}{2k_1 k_2 - k_2^2 + 1} \quad (k_1 = -ctg\theta, \theta = \arcsin NA, k_2 = -4Am) \quad (7)$$

$$m = \frac{ctg\theta - \sqrt{ctg^2\theta - 8A(rctg\theta + d - AR_B^2)}}{4A} \quad (8)$$

$$n = -mctg\theta + rctg\theta + d \quad (9)$$

4. Calculation Results and Analysis

According to the mathematical model above, by calculating them respectively, the influences on the sensors from the structural parameters of optical fiber bundle such as the initial distance d between the optical fiber and the diaphragm, the radius r of the two optical fibers, the distance l between the two optical fibers are found, and the light intensity modulation function curve when variables change is drawn.

As is shown in figure 6 and figure 7, when variable d respectively is $150\mu m, 200\mu m, 250\mu m, 300\mu m$ (l is $20\mu m$, r is $50\mu m$, NA is 0.5 , A is 0.04×10^{-7} , R_1 is $5mm$), the curve P—M can be got. In figure 8 and figure 9, when variable r respectively is $45\mu m, 50\mu m, 55\mu m, 60\mu m$ (l is $20\mu m$, d is $250\mu m$, NA is 0.5 , A is 0.04×10^{-7} , R_1 is $5mm$), the curve P—M can be got. In figure 10 and figure 11, when variable l is $15\mu m$ ($130\mu m$), $18\mu m$ ($136\mu m$), $21\mu m$ ($142\mu m$), $24\mu m$ ($148\mu m$) (r is $50\mu m$, d is $250\mu m$, NA is 0.5 , A is 0.04×10^{-7} , R_1 is $5mm$), the curve P—M can be got.

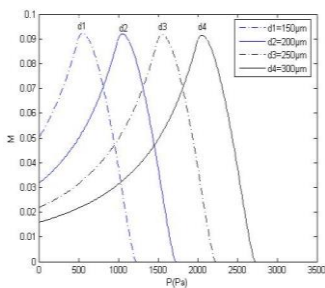


Figure 6. The P — M Fig of d Changes in (2)

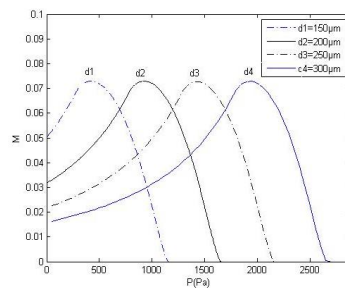


Figure 7. The P — M Fig of d Changes in (6)

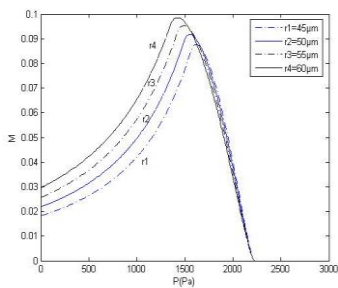


Figure 8. The P — M Fig of r Changes in (2)

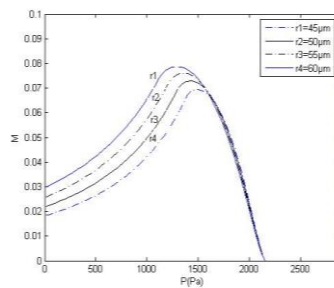


Figure 9. The P — M Fig of r Changes in (6)

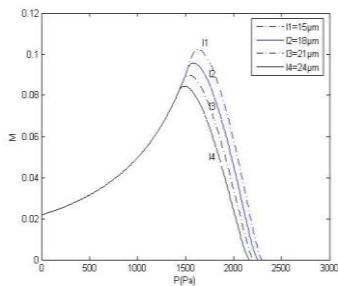


Figure 10. The P — M Fig of l Changes in (2)

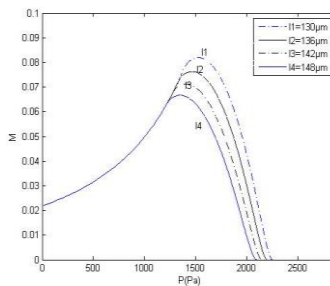


Figure 11. The P — M Fig of l Changes in (6)

It is not difficult to see that the initial output light intensity ratio is greater when the value of d is small, and the elastic diaphragm is near the optical fiber. Meanwhile, when the value of d is certain, with the increase of pressure P , the distance between the elastic diaphragm and the optical fiber becomes smaller gradually, which makes the output light intensity first increase and then decrease. With the change of the fiber core radius, the change of the fore slope curve width is not obvious, but with the increase of the fiber core radius, the peak value of the curve is increasing slightly. With the change of the distance l , the change of the fore slope curve width is not much, and has little influence on the detection range of the pressure P . With the increase of the distance l , the peak value of the curve will decrease. The analysis result above is consistent with the actual situation.

By comparing formula (2) with formula (6), it is not difficult to find that the two kinds of curves have similar variation trends—both of them increase firstly and then decrease. When the structural parameters of the two typical optical fiber bundle are the same, the variation range of the corresponding pressure P is nearly the same. This means that detection range of the pressure is nearly the same about the two optical fiber structure, but the peak value of the curve is different, and the peak value in formula (2) is about 18 % bigger than that in formula (6).

According to the analysis results of the two typical fiber distribution structures above, it can be found that the pressure detection range and the detection sensitivity of the two kinds of sensor have little differences. Considering that the coaxial distribution structure of the incident optical fiber and the reflector is easy to achieve, and is conducive to the latter theoretical analysis and calculation, the coaxial designing forms that the

incident fibers and many receiving fibers are getting together into bundles are recommended in the actual production of the sensor. In the practical application of RIM—FOS, people mostly adopt this kind of fiber bundle as light transmission channel.

5. Conclusion

This paper has done the theoretical research of the cured surface reflection RIM-FOS under the typical optical fiber beam structure, and has researched the intensity modulation model of the typical fiber bundle structures such as fiber's axial symmetry distribution and fiber's coaxial distribution, and so on. Under the fiber's axial symmetry distribution structure, the intensity modulation model of the cured surface reflection RIM-FOS can be simplified as formula (2) in the article. Under the fiber's coaxial distribution structure, the intensity modulation model of the cured surface reflection RIM-FOS can be simplified as formula (6) in the article. Then the corresponding curves P—M of the two kinds of distribution structures can be got when the structural parameters such as d , r , t , etc change by using computer soft wares. Through the calculated results, it's found that the pressure detection range are nearly the same under the two kinds of fiber bundles structures when the structural parameters are designed the same, and the peak value of the curves are different slightly. This means that the pressure detection range and the detection sensitivity of the two typical fiber bundle structures are similar. In order to design and calculate conveniently, in the practical designing of RIM—FOS, it should adopt the coaxial designing forms that the incident fibers and many receiving fibers are getting together into bundles.

Acknowledgments

Joint fund in science and technology department of Guizhou Province (LKG[2013]39); Science and technology cooperation plan of Guizhou Province (LH[2015]7660); The introduction of talent fund of Guizhou University ((2014)43).

Reference

- Brandao-Faria J.A., 2000, Modeling the Y-branched optical fiber bundle displacement sensor using quasi-Gaussian beam approach, *Microwave and Optical Technology Letters*, 25,138-141
- Erik A. M., Michael D.T., Anthony D.P., 2012, Performance optimization of bundled fiber optic displacement sensors, *Proc SPIE , Smart Sensor Phenomena, Technology, Networks, and Systems Integration*, 8346,1112-1117
- Faria J.B., 1998, A theoretical analysis of the bifurcated fiber bundle displacement sensor, *IEEE Transactions on Instrumentation and Measurement*, 47,742-747
- García Y.R., Corres M.J., Goicoechea J., 2010, Vibration Detection Using Optical Fiber Sensors, *Journal of Sensors*, 1-12. Doi: 10.1155/2010/936487
- Nevshupa R., Conte M., Rijn v.C., 2013, Measurement uncertainty of a fiber-optic displacement sensor, *Measurement Science and Technology*, 24, 510-514
- Puangmali P., 2010, Mathematical Modeling of Intensity-Modulated Bent-Tip Optical Fiber Displacement Sensors, *Instrumentation and Measurement*, 59, 283-291. Doi: 10.1109/TIM.2009.2023147
- Puangmali P., 2011, Modeling of Light Intensity-Modulated Fiber-Optic Displacement Sensors, *Instrumentation and Measurement*, 60, 1408-1415
- Zawawi A.M., O'Keffe S., Lewis E., 2013, Intensity-modulated fiber optic sensor for health monitoring applications: a comparative review, *Sensor Review*, 33, 57-67
- Zheng J.I., Albin S., 1999, Self-referenced reflective intensity modulated fiber optic displacement sensor, *Optical Engineering*, 38,227-232